Int J Clin Exp Pathol (2009) 2, 339-352
www.ijcep.com/IJCEP810008

Original Article

Cortical Neurons Transgenic for Human Aβ40 or Aβ42 Have Similar Vulnerability to Apoptosis despite Their Different Amyloidogenic Properties

Najeeb A. Shiwany, Jun Xie and Qing Guo

Department of Physiology, University of Oklahoma Health Sciences Center, Oklahoma City, OK 73104

Received 23 October 2008; Accepted 26 October 2008; Available online 26 November 2008

Abstract: Alzheimer's disease (AD) is a leading cause of chronic dementia in the United States. Its incidence is increasing with an attendant increase in associated health care costs. Amyloid β peptide (Aβ; a 39-42 amino acid molecule) is the major component of senile plaques, the hallmark lesion of AD. The toxic mechanism of Aβ peptides has not been well characterized. Specifically, the impact of Aβ1-40 (Aβ40) and its slightly longer counterpart fragment, Aβ1-42 (Aβ42), is not clearly understood. It has been suggested that, while Aβ40 might play a more physiologically relevant role, Aβ42 is likely the key amyloidogenic fragment leading to amyloid deposition in the form of plaques in AD, a pivotal process in Alzheimer's pathology. This notion was further supported by a recent study employing transgenic mouse models that expressed either Aβ40 or Aβ42 in the absence of human amyloid beta protein precursor (APP) overexpression. It was found that mice expressing Aβ42, but not Aβ40, developed compact amyloid plaques, congophilic amyloid angiopathy, and diffuse Aβ deposits. Since neuronal loss is one of the hallmark features in AD pathology, we hypothesize that cortical neurons from these two strains of transgenic mice for Aβ might show different vulnerability to cell death induced by classical inducers of apoptosis, such as trophic factor withdrawal (TFW). Contrary to our expectations, we found that, while overexpression of either Aβ40 or 42 significantly increased the vulnerability of primary cortical neurons to WFT-induced cell death, there was no significant difference between the two transgenic lines. Mitochondrial dysfunction, levels of oxidative stress, caspase activation and nuclear fragmentation are increased to about the same extent by both Aβ species in transgenic neurons. We conclude that Aβ40 or Aβ42 induce similar levels of neurotoxicity following TFW in these transgenic mice despite the difference in their amyloidogenic properties.

Keywords: Alzheimer's disease, amyloid beta-peptide, transgenic mouse model, cortical neurons, cell death, trophic factor withdrawal

Introduction

Dr. Alois Alzheimer, a Bavarian psychiatrist, interviewed a patient in 1901. This was a 51 year-old woman who had declining cognitive abilities and memory. Her neurological evaluation by Alzheimer, Emil Kraeplin and others first helped define this clinicopathological syndrome of late-life mental decline [1]. However, it was not until the 1960s that the work of Tomlinson *et al* established Alzheimer's disease (AD) as the most common form of senile dementia [2-4]. Today, with exponential advances in fields such as neurology, pathology, biophysics, computer modeling, molecular genetics and immunochemistry, many aspects of AD, its etiology and underlying mechanisms have been discovered. However, a robust scientific debate still continues about the fundamental mechanistic details of the disorder. It's not surprising therefore, that a cure has yet to be discovered, even in the face of an increasing health care burden and near epidemics of the disease in the United States and across the western hemisphere. Amyloid plaque deposition in specific areas of the brain is a hallmark feature of AD. Such deposition is thought to occur as a consequence of aberrant amyloid precursor protein (APP) proteolysis by β- and γ-secretase enzymatic activity leading to increased synthesis of the amyloid beta-peptide (Aβ 1-42 or Aβ 1-40) fragments of APP. Aβ is deposited in the extra-neuronal

space in the AD brain. Through as yet unidentified mechanisms, Aβ seems to lead to neuronal dysfunction and degeneration, as well as synaptic loss. Although Aβ40 is likely a physiologically relevant molecule and tends to be less amyloidogenic, Aβ42 is highly amyloidogenic and seems to be a major component of the amyloid plaques. Because these pathologies (amyloid plaques and neurofibrillary tangles) appear to manifest in sub-cortical areas that are involved in memory and cognition (temporal lobe, parietal lobe, parts of the frontal cortex and cingulate gyrus) [5], the AD clinical phenotype is predictably one of progressive memory loss, cognitive decline and personality change. Even though these abnormalities have been studies for decades, the exact underlying mechanism of Aβ toxicity remains elusive.

The search for an effective non-human AD research model also continues and is likely to be critical to our understanding of the pathophysiology of Aβ peptides in AD. Traditionally, overexpression of AD-linked mutant APP has proven most effective in simulating Aβ deposition in the rodent brain [6]. However, the confounding potential of APP overexpression remains a concern in this strategy. For example, excess APP results in overproduction of APP fragments and these peptides might have both neuroprotective as well as neurotoxic properties [5, 7, 8]. In addition, there is evidence that the APP intracellular domain may have signaling functions that could prove confounding [9]. Therefore, mice that overexpress individual Aβ peptides without an attendant change in APP levels would allow us to test a variety of hypotheses aimed at clarifying the role of these fragments both in the process of amyloid deposition and the generation of an AD-like phenotype. This tactic was recently used and the results published by a Mayo clinic group in Jacksonville, FL [6]. In this transgenic model, overexpression of human Aβ42 (in contrast with overexpression of human Aβ40) were shown to accumulate insoluble Aβ42, develop compact amyloid plaques, congophilic amyloid angiopathy and diffuse Aβ deposits in the brain. These results point to a potentially different mechanism of action for Aβ40 and Aβ42 in the pathogenesis of AD. Given the highly amyloidogenic property of Aβ42, and the previously published data on the neurotoxicity of amyloid plaques, it seems to be reasonable to assume that, under challenged conditions (such as trophic factor withdrawal), cortical neurons from mice overexpressing Aβ1-42 would have the greatest propensity for death when compared with neurons derived from animals overexpressing Aβ1-40. If production of Aβ by cleavage of APP via beta- and gamma-secretases is considered a largely pathogenic process, it could also be hypothesized that neurons from the wild-type (WT) animals under exactly the same conditions would be more resistant to cell death than those overexpressing human Aβ.

Several lines of evidence strongly suggest that activation of apoptotic pathways contributes to neuronal loss in AD. For example, results from post-mortem brain tissue of AD patients indicate that apoptosis had occurred in these brain specimens [10]. Changes in mitochondrial transmembrane potentials are also an intrinsic part of the classic apoptotic machinery of cell death and therefore would be expected to occur in AD [11]. Oxidative stress by hydrogen peroxide or hydroxyl radicals may also induce apoptosis *in vitro* [12]. Using the same transgenic mouse models developed by McGowan and colleagues, we found that, contrary to our initial expectations, there were no significant differences in cell death between Aβ1-40 and Aβ1-42-derived cortical neurons in primary culture under classical apoptotic conditions of trophic factor withdrawal (TFW), although neurons transgenic for either forms of Aβ showed significantly increased vulnerability to TFW-induced apoptosis compared with non-transgenic control neurons. These results suggest that Aβ40 and Aβ42 have similar neurotoxic properties even though their amyloidogenic properties are significantly different.

Materials and Methods

All experimental procedures and animal use were approved by the Institutional Animal Care and Use Committee of the University of Oklahoma Health Sciences Center (OUHSC).

Mice

Experiments were performed on primary cortical neurons derived from one-day-old pups from a breeding colony of BRI-Aβ40 (designated Aβ40), BRI-Aβ42 (designated Aβ42) and Tg2576 (designated WT) mice.

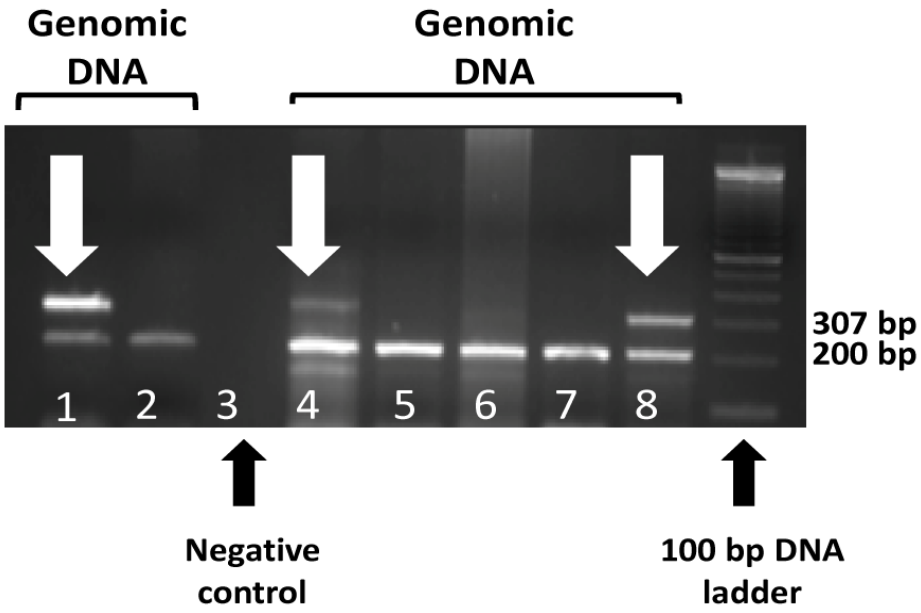

Figure 1 BRI-Aβ/BRI-Aβ42 genotyping. Individual lanes were loaded with a PCR amplicon of genomic DNA isolated from tail clippings of 1-day-oldmouse pups. Lanes 1 and 2 and 4 through 8 are sample lanes. Lane 3 is a negative control. Lanes1, 4 and 8 exhibit the characteristic double band (307 and 200 bp) of the heterozygous BRI-Aβ transgene (this is an example of Aβ40). The single bands corresponding to 200 bp in lane 2 and lanes 5 through 7 are from WT DNA.

These transgenic mice were generated and maintained on a B6C3 background. The colony was established at the Comparative Medicine Animal Facility of OUHSC and was itself derived from breeding pairs generously gifted by Dr. Eileen McGowan of the Mayo Clinic College of Medicine, Jacksonville, FL. Details of derivation technique and related information about the transgenic mice have been described previously [6].

Cell Culture

Dissociated cultures of cortical neurons were prepared from postnatal day 1 mouse pups (Aβ40, Aβ42 and WT) using methods described in our previous studies [13]. Briefly, cortices were removed and incubated for 15 min in Ca^{2+} and Mg^{2+} free Hank's balanced saline solution (Invitrogen) containing 0.2% papain. Cells were dissociated by trituration and plated into polyethyleneimine-coated glass-bottom culture dishes containing Minimum Essential Medium with Earle's salts supplemented with 10% heat-inactivated fetal bovine serum, 2mM L-glutamine, 1mM pyruvate, 20mM KCL, 10mM sodium bicarbonate and 1mM Hepes pH7.2. Following cell attachment (3-6h post-plating), the culture medium was replaced with Neurobasal growth medium with B27 supplements (Invitrogen). Plated cells were allowed to grow for 7 days before they were subjected to TFW.

Genotyping

Transgenic mouse pups used in our experiments were born to heterozygous parents with the specific allele expressing either as a neuronal overexpression of Aβ40 (BRI-Aβ40) or Aβ42 (BRI-Aβ42). The genotyping method was modified from the original provided by Dr. Eileen McGowan [6]. Briefly, genomic DNA was extracted from preserved mouse tail clippings (stored at -80° after harvest) using the DNeasy® extraction kit (QIAGEN). For both Aβ40 and Aβ42, the forward primer used for the PCR reaction was common (5'-AAGGCTGGAACCTATTTGCC-3'). For reverse primers, Aβ40 and Aβ42 had specific primer constructs (Aβ40: 5'-CGTTACTAGTGGATCCCTAG-3'; Aβ42: 5'-TAGTGGATCCCTACGCTATG-3'). For PCR internal controls the following primer constructs were used: Forward 5'-CAAATGTTGCTTGTCTGGTG-3'; Reverse 5'-GTCAGTCGAGTGCACAGTTT-3'. PCR master mix was constituted from the QIAGEN Taq DNA

polymerase kit. PCR conditions were: denaturation 1 cycle at 94°C for 3 minutes; amplification for 3 cycles at 94°C for 10 seconds, 59°C for 15 seconds and 72°C for 30 seconds (amplification for 35 cycles); 72°C for 5 minutes and then hold at 4°. The PCR amplicon was then run on a 2% agarose gel in TBE buffer for 2 hours at 120V DC current using a standard electrophoretic apparatus. The gel was imaged under UV light to identify DNA bands corresponding with transgenes or WT alleles in the sample. A single band (**Figure 1**) at 200 bp corresponded with the internal control while this band and a second at 307 bp identify the BRI-Aβ transgene.

Mitochondrial Transmembrane Potential Assay

The dye Rhodamine 123 (Rhd123, Invitrogen) was used to measure mitochondrial transmembrane potential by employing methods similar to those described previously [14]. Briefly, cells were incubated for 30 min in the presence of 10μM Rhd123 and wash twice in Locke's solution (154mM NaCl, 5.6mM KCl, 2.3mM $CaCl_2$, 1mM $MgCl_2$, 5mM $NaHCO_3$, 3.6mM glucose, and 5mM HEPES, PH7.2). Cellular fluorescence was visualized using a Nikon Eclipse TS100 fluorescence microscope with excitation at 488nm and emission at 510nm. Images were captured using a Nikon digital DXM 1200F camera and acquired, processed, and analyzed with Nikon ACT-1 software.

Caspase-3 Assay

1-week-old cortical neuronal cultures were used to quantify caspases-3 activation. Briefly, the assay was performed by the release of 7-amino-4-trifluoromethyl-coumarin (AFC) from DEVD-AFC. 50 μl of 2X reaction buffer containing 10mM DTT was added to culture plates. 5 μl of DEVD-AFC was added to each plate followed by incubation at 37°C for 2 hours. Following incubation, PBS buffer was used to rinse the plates 2-3 times before examination under a fluorescent microscope (emission spectra imaged at 505 nm). Images were captured by a Nikon microscopic image capture system and analyzed off line.

Measurement of Intracellular Peroxide Level

Peroxide levels were measured by using the 2,7-dichlorofluorescein diacetate (H2DCF) dye. This molecular probe easily penetrates cellular membranes and is hydrolyzed intracellularly to the essentially non-permeant H2DCF which is non-fluorescent but becomes oxidized to fluorescent and non-permeant dichlorofluorescein (DCF). Briefly, cells were incubated for 20min in the presence of 50μM H2DCF, followed by washing in Hanks' balanced saline solution containing 10mM Hepes buffer and 10mM glucose. Cells were imaged by a Nikon fluorescent microscope. Values of cellular fluorescence (average pixel intensity per cell) were obtained with the software supplied by ACT-1.

Measurement of DNA Fragmentation

Propidium Iodide (PI) is a membrane-impermeant dye. Permeation of cultured neurons was achieved by aspirating growth medium and exposing them to 0.2% Triton X-100 in PBS buffer for 20 minutes followed by three washings with buffer alone. Once inside the cell, it stains DNA and RNA by intercalating into nucleic acid molecules. In our experiments, neuronal cultures were incubated with 5uM propidium Iodide for 20min. Levels of PI flurorescence were visualized by Nikon TS-100 fluorescence microscope and images were captured using a Nikon digital DXM 1200F camera and analyzed with Nikon ACT-1 software. At least 100 cells per culture from six random microscopic fields of view at x200 magnification were counted, and counts were made in at least six separate cultures per treatment condition. Cells exhibiting nuclear chromatin condensation and fragmentation are counted as apoptotic cells.

Cell Death Count

Cortical cell cultures were established from 1-day-old embryos using methods outlined above. Cells were grown in polyethyleneimine-coated plastic or glass bottom 35 mm culture dishes containing Eagle's Minimum Essential Medium supplemented with 10% (v/v) heat-inactivated fetal bovine serum (Life Technologies, Gaithersburg, MD), 20 mM KCl, and 1 mM pyruvate. The atmosphere consisted of 6% CO_2/94% room air and was maintained near saturation with water. Experiments were performed in cultures that had been maintained for 7 days. Cells were evaluated before, 4, 8, 24 and 48 hours after TFW challenge. Neuronal viability was assessed by

morphological criteria; cells with intact neurites of uniform diameter and a soma with a smooth round appearance were considered viable, whereas neurons with fragmented neurites and a vacuolated or swollen soma were considered nonviable. Analyses were done without knowledge of the treatment history of the cultures.

Data Analysis

Statistical differences between experimental groups were determined by performing one-way ANOVA followed, by post-hoc Tukey's test for multiple comparisons against a control group. Data is reported as mean ± SEM. Results were considered significant at a p value <0.05.

Results

Sensitivity to TFW challenge was evaluated by measuring DNA damage, changes in mitochondrial transmembrane potential, levels of oxidative stress and apoptosis quantification.

TFW Provokes Significantly more DNA Fragmentation in Abeta Transgenic Neurons than in WT Neurons.

Using nuclear fragmentation as a criterion of apoptotic cell death, we examined the effect of TFW challenge on the survival of cortical neurons derived from Aβ40, Aβ42 and WT pups. Specifically, by using PI DNA intercalating fluorescent probe, we documented fragmentation of nuclear DNA over time when cells were exposed to glucose free Locke's medium. We studied two time points; 2 hours and 24 hours post-challenge. At 2 hours post-challenge, cells were counted using the PI probe to identify cell nuclei. Raw counts were performed of positively identified

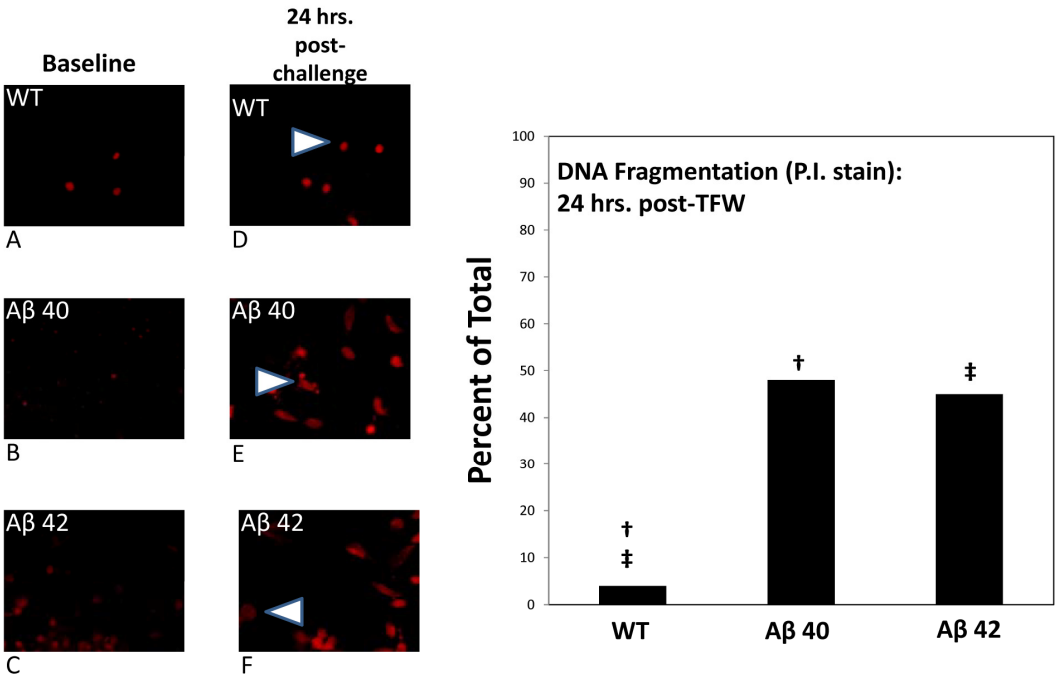

Figure 2 Propidium Iodide staining in 1-week-old cortical neuronal cultures. 1-week-old cortical neuronal cultures were challenged by TFW. At various time points following TFW challenge, culture plates were exposed *in vitro* to Propidium Iodide. The fluorescent signal from the DNA intercalating dye was imaged and stored for off line analysis. Panels **A**, **B** and **C** are representative images from WT, Aβ40 and Aβ42 cortical neurons respectively after 1 week of culture and under basal conditions of TFW challenge. Panels **D**, **E** and **F** are corresponding images at 24 hours post-TFW challenge. In **D**, **E** and **F**, arrowheads identify typical morphology of "speckled" or "rough" staining of nuclei and are markers for DNA fragmentation. The right half of the figure is a bar plot showing the fraction of cells (% of total counted in all fields) that had this "fragmented" morphology. WT are compared with Aβ40 and Aβ42. WT neurons had 4% fragmentation while Aβ40 exhibited 48% and Aβ42 displayed 45% speckling or fragmentation. Both transgenic groups had a statistically significant result when compared with WT (p = <0.05). However, when the transgenic neurons were compared with each other, no statistical significance was observed.

neurons in all available microscopic fields and the number of nuclei that had a smooth appearance (where the fluorescent probe had evenly intercalated with the nuclear DNA) was determined. Further, in every microscopic field, speckling of the fluorescing nuclear material was visualized and this was the determinant of the second population of cells that were labeled as exhibiting DNA fragmentation. This process was repeated for the second time point (24 hours post-challenge). The percentage ratio of speckled-to-smooth cells was used to plot the data (**Figure 2**). At 2 hours after TFW challenge, none of the cells examined had evidence of speckling/DNA fragmentation. At 24 hours of TFW challenge, only a very small fraction (4%) of WT neurons had evidence of DNA fragmentation. However, 48% of Aβ40 and 45% of Aβ42 neurons appeared to have evidence of DNA fragmentation. This was also statistically significant in comparison with WT cell counts. Thus there was evidence of sharply elevated DNA damage consistent with apoptotic morphology in both transgenic cell types compared with WT control neurons following WFT.

Mitochondrial Transmembrane Potential is Disrupted as an Early Event after TFW Challenge in Transgenic Compared to WT Neurons.

To assess differential mitochondrial function in WT and transgenic neurons, the cationic, cell permeant, green-fluorescent dye Rhd123 was used as a probe. Rhd123 is selectively sequestered in active mitochondria and is used as a marker for mitochondrial transmembrane potentials. Following TFW challenge of cultured neurons, Rhd123 probe was used to assess mitochondrial dysfunction at various time points (0, 4, 8 and 24 hours) after challenge. The data was mean

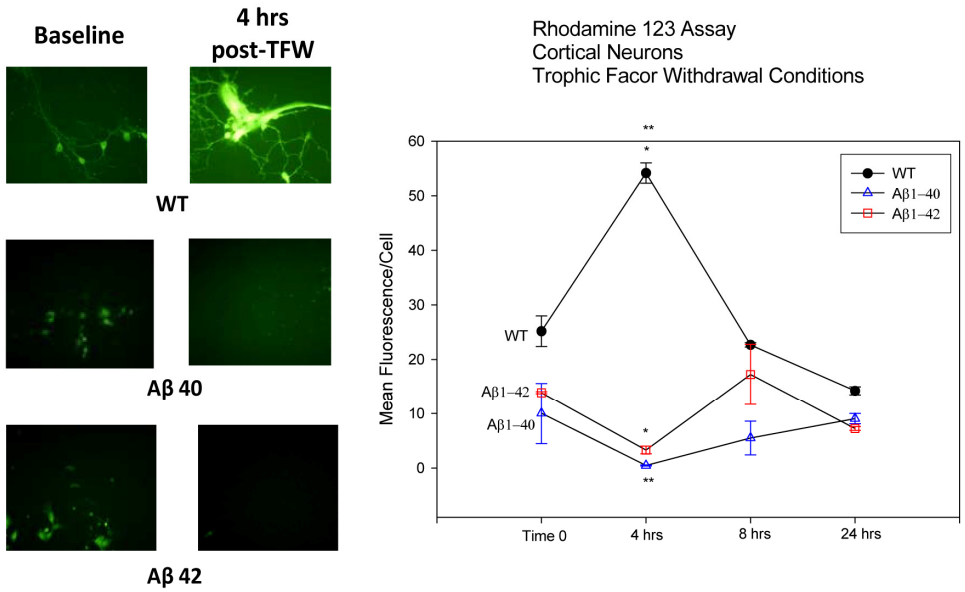

Figure 3 Rhodamine 123 sequestration as a function of mitochondrial transmembrane potential. 1-week-old cortical neuronal cultures were challenged with TFW. At various time points after challenge (0 hrs, 4 hrs, 8 hrs and 24 hrs), culture plates were then exposed *in vitro* to the fluorescent mitochondrial probe, Rhodamine 123. The fluorescent signal from culture plates was imaged with photomicroscopy at 510 nm emission spectrum and analyzed off line. The images were evaluated using an image analysis software with fluorescent intensity quantified in arbitrary units. This analysis was finally utilized to plot the line graph (right half of the figure), displaying average fluorescent intensity per cell ± SEM. The images in the left half of the figure represent baseline activity (time 0 of TFW challenge) and 4 hours after TFW challenge (the time observed to have the most significant change from baseline levels). The three panels on the left (top, middle and bottom) are representative of baseline conditions for the three cell types (WT, Aβ40 and Aβ42). The panels on the right (top, middle and bottom) represent 4 hours post-TFW challenge. Statistical significance was observed between WT neurons and the transgenic cells at 4 hours post TFW challenge (p = <0.05). At this time point, differences between the two transgenic neuronal cultures did not reach statistical significance.

fluorescence in arbitrary units per cell as analyzed by offline image processing using commercial software. Immediately after TFW challenge, Aβ40 and Aβ42 neurons were observed to have a slightly lower Rhd123 fluorescence in comparison with WT cells. At 4 hours, Rhd123 fluorescence was significantly increased in WT neurons while attenuated in both transgenic cell lines. However, there was no difference in the fluorescent intensity between the Aβ40 and Aβ42 groups. When WT cells were compared with transgenic neurons, a statistically significant result was obtained (**Figure 3**). Although, Rhd123 fluorescence appeared to increase somewhat at later time points following TFW (8 and 24 hours), this increase was very small and was not statistically significant. Overall, WT cells appeared to have increased mitochondrial transmembrane potentials shortly after TFW (possibly reflecting compensatory mitochondrial activity under nutritive challenge in order to synthesize more ATP). This compensatory spike was not noted in either Aβ40 or Aβ42, suggesting that they were less able to compensate for the nutritive challenge.

Caspase-3 Activation is Upregulated at Basal Levels and Peaks at 8 Hours post-TFW Challenge in Transgenic Compared to WT Neurons.

We used the DEVD-AFC-based assay for activated caspase-3 detection under TFW conditions in the three neuronal populations. Under basal conditions (time 0 post-TFW), all three cell types (WT, Aβ40 and Aβ42) demonstrated no caspase-3 activation (**Figure 4**). Following TFW challenge, caspase-3 activation started to increase, reaching a peak value at 8 hours post-challenge. This increase was largely parallel between the three neuronal populations with Aβ42 cells exhibiting the highest level of activity, Aβ40

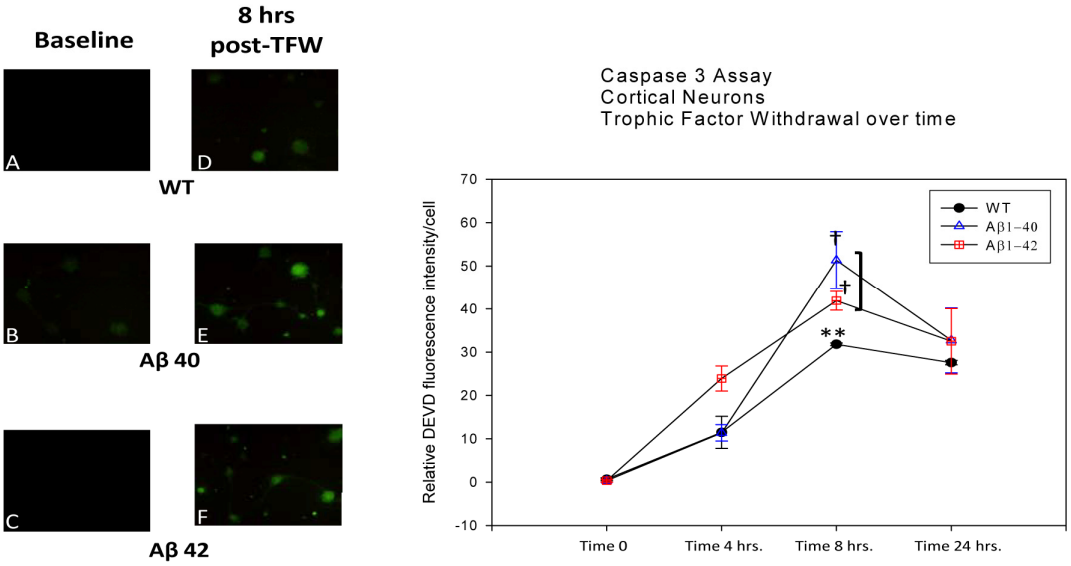

Figure 4 Casapse 3 activation following TFW challenge. 1-week-old cortical neuronal cultures were exposed to TFW. At various time points following challenge (0, 4, 8 and 24 hrs), culture dishes were processed following a DEVD-AFC-based caspase-3 activation protocol. Fluorescent images were analyzed with a Kodak image analysis software which measures average pixel intensity per cell (these data was subtracted from average pixel intensity of adjacent background). Data was analyzed as the means of the differences between intensity per cell and background intensity. Panels **A**, **B** and **C** on the left of the figure are representative of caspases-3 activation at basal levels (0 hr post-TFW challenge). Panels **D**, **E** and **F** are representative of caspases-3 activation at 8 hrs post-challenge (the time point where the most marked change in activity was noted). The line plot on the right displays relative DEVD fluorescence per cell (as a marker for activation of caspases-3). Data points are average fluorescent intensities of all cells observed per microscopic field ± SEM. WT, Aβ40 and Aβ42 neurons are compared at 0, 4, 8 and 24 hrs after onset of TFW. At basal levels (0 hrs), there is virtually no caspase-3 activation. As time progresses a significant point is reached at 8 hrs. The two transgenic cell types appear significantly different in caspases-3 activation compared to WT neurons while remaining similar in comparison with each other (p = <0.05).

cells showing somewhat intermediate activity, while WT neurons displaying the lowest level of activity over time. Finally, at 24 hours post-TFW challenge, caspase-3 activation began to attenuate for all three populations reaching levels approximately intermediate between those observed at 4 and 8 hour time points. There was a statistically significant difference in caspase-3 activation at time 8 hours after TFW conditions were initiated (**Figure 4**). However, at 4 hours and 24 hours after TFW exposure, no statistically significant difference was noted between Aβ40, Aβ42 and WT neurons.

Oxidative Stress is Higher at 8 and 24 Hours post-TFW Challenge in Transgenic Neurons than in WT Neurons.

When 1-week-old cortical neurons from WT and transgenic pups were exposed to TFW challenge, differences in oxidative stress began to emerge. Oxidative stress was measured by the oxidative conversion of H2DCF to the fluorescent DCF by H_2O_2. At basal levels (time 0 after onset of TFW), all three cell types (WT, Aβ40 and Aβ42) remained comparably quiescent. However as time progressed following nutritive challenge, oxidative stress increased in lock-step up to 4 hrs after TFW onset (**Figure 5**). Thereafter, transgenic cell (both Aβ40 and Aβ42) H_2O_2 activity appeared to increase and diverge from that seen in WT neurons. WT cells remained close to basal activity levels throughout the measurement time points (0, 4, 8 and 24 hrs.). Indeed, at both 8 and 24 hrs after TFW challenge, mean levels of DCF fluorescence intensity in transgenic neurons were noted to be significantly higher than those in WT neurons ($p = <0.05$). However at each of these later time points (8 and 24 hrs.), there was no significant difference between the two transgenic neurons.

Transgenic Cortical Neurons Exhibit more Vulnerability to Apoptotic Cell Death 24 to 48 Hours after TFW Challenge Compared with WT.

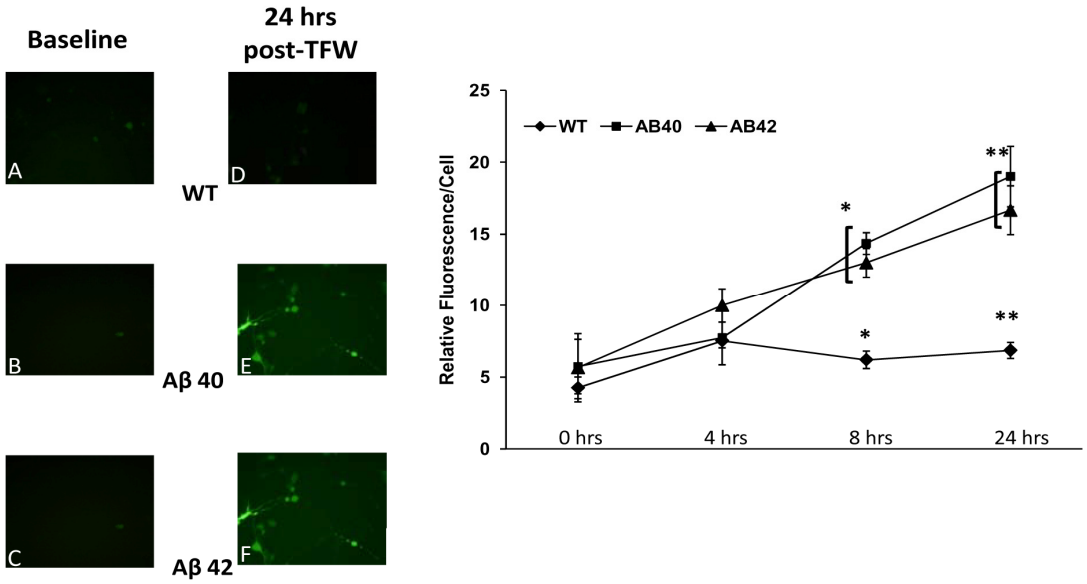

Figure 5 Oxidative Stress in 1-week-old cortical neuronal cultures measured by DCF fluorescence. Cortical neurons in culture following 1 week of conditioning were exposed to TFW conditions. At various time points following nutritive challenge (0, 4, 8 and 24 hrs), cultured plates were processed for DCF fluorescence analysis as a measure of H_2O_2 activity. At 0 and 4 hrs post challenge, there was no difference in activity between the three neuronal types (WT, Aβ40 and Aβ42). However, there was a uniform increase in oxidative stress at 4 hrs compared to 0 hrs. At 8 hrs, significant differences began to emerge between the three groups of cultured cells. While WT levels of DCF fluorescence remained somewhat stable at roughly the levels seen at 4 hrs, both transgenic neurons began to show heightened stress and this continued at 24 hrs as well. At these two later time points (8 hrs and 24 hrs) both transgenic neurons had statistically significant amplification of oxidative stress (i.e. DCF fluorescence) compared with WT ($p = <0.05$). However, at both these later time points the two transgenic neuronal cultures were essentially equal in oxidative stress with somewhat higher levels recorded at 24 hrs compared to 8 hrs after TFW challenge.

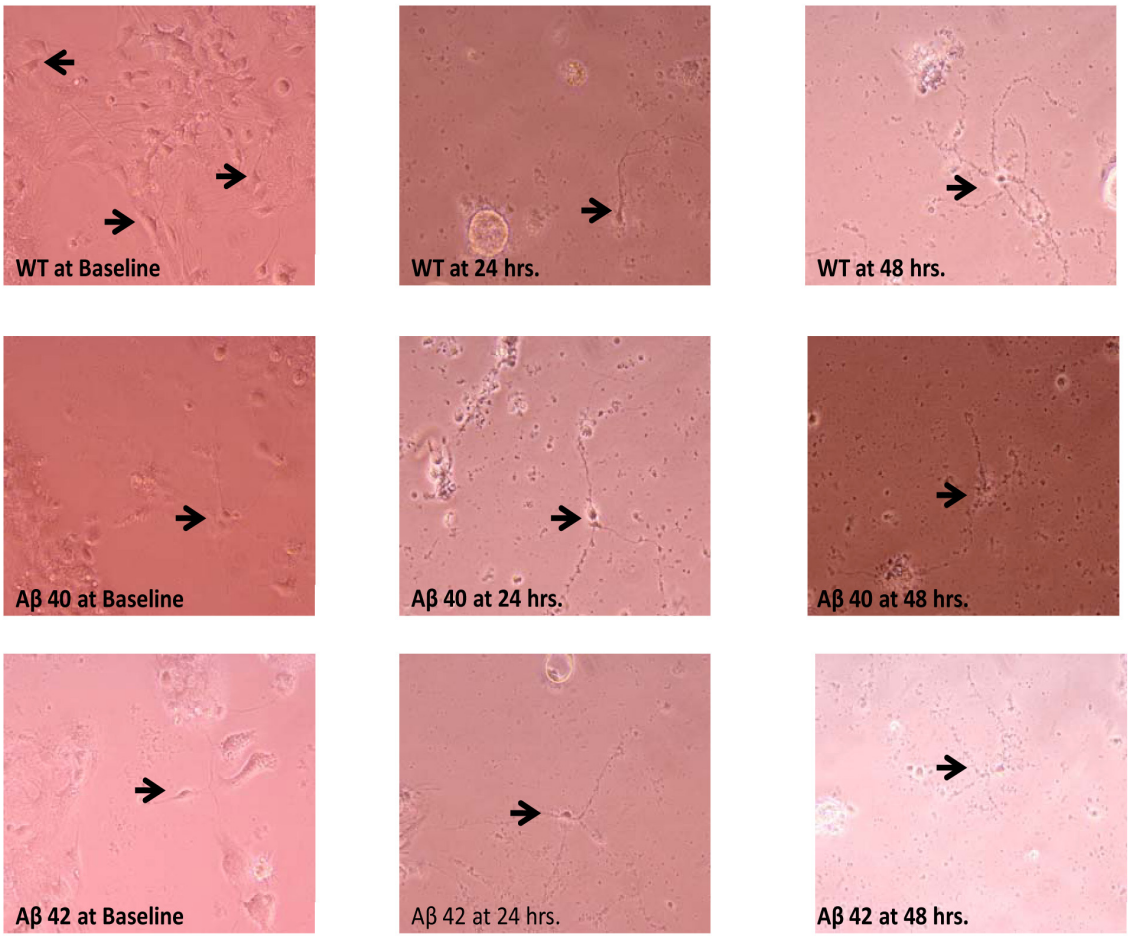

Figure 6 Cortical neuronal cultures (unstained) at various times following TFW challenge. Conditioned 1-week-old cortical neuronal cultures form 1-day mouse pups were exposed to TFW. Phase contrast images at various time points were obtained (Baseline or 0 hr, 24 hrs and 48 hrs). There was a progressive evolution of apoptotic morphology in cultured cells. This was most marked in the transgenic population (Aβ40 and Aβ42) and somewhat less so in WT. At 24 hours in particular (middle column of images), WT cells exhibited fewer or less robust apoptotic features than either Aβ40 or Aβ42 cells. At 48 hours post challenge, all three populations had become grossly apoptotic.

We sought to document direct evidence of apoptotic cell death (the presumed dominant process in AD neuronal loss). This was achieved by following the three neuronal populations (WT, Aβ40 and Aβ42) over various time points following TFW challenge. These cultured populations were then photographed under phase-contrast microscopy and morphologic criteria (as outlined above) were sought. At basal levels following TFW (0 hours), all three cell cultures were observed to be in good health. At 24 hours of nutritive challenge, both transgenic neuronal isotypes had begun to exhibit typical features of cell death. Interestingly, at this time point WT neurons showed the least amount of cell death with fewer or less remarkable cell death morphology. However, after 48 hours of the onset of TFW conditions, such differences were all but lost and all three cultured populations had become apoptotic (**Figure 6**).

Discussion

While many details of the AD pathogenesis have been elucidated, several fundamental questions remain unanswered. It has been established, for example, that AD is a "triple amyloidosis". This term refers to the fact that the AD brain (sporadic or familial) manifests pathological fibrillization of at least three peptide types: Aβ, τ and α-synnuclein [15]. These three types of peptides accumulate in the AD brain as three distinct lesions: amyloid

plaque (AP), neurofibrillary tangles (NFT) and Lewy Bodies (LB). Even if one considers only amyloid plaques, the picture appears significantly complex. For example, even though it has been known for some time that Aβ42 levels are elevated in the AD brain, it is also evident that plaques vary in protein composition, both in terms of the types of Aβ peptides and of other proteins found in them [16]. In addition, a variety of other substances are also known to accumulate in these lesions [17, 18]. Thus, it has been difficult and challenging to tease out mechanistic details of AD pathogenesis.

It is particularly problematic to clearly understand the individual role of the two key peptides Aβ40 and Aβ42, which are the central players in the neuropathology of AD. These peptides are normally cleaved from the precursor APP molecule in a roughly 9:1 ratio [19]. This ratio appears to change in the sense that extracellular levels of Aβ42 increase and, this in turn, leads to deposition of these and other molecules as plaques [20].

AD does not appear to be a uniquely human disorder. Certain non-human mammalian species exhibit neuropathology which is strikingly similar to AD and these include non-human primates and canines [21]. However, in rodents where AD is most commonly studied, sporadic age-related amyloid plaques do not occur. Thus there is a reliance on artificially inducing this anomaly in rodent brains and the only reliable manner in which this strategy can be implemented is by overexpressing human APP transgenes [6]. This is a significant confounder since some proteolytic fragments of APP have inherent neuroprotective or neurotoxic properties and the APP intracellular domain seems to have cell signaling functions [7-9]. Therefore, the creation of the BRI-Aβ1-40 and BRI-Aβ-42 transgenic mouse strains will likely prove to be a novel tool [6]. This is the model we chose to use to evaluate some fundamental mechanistic ideas on Aβ pathophysiology in a neuronal cell culture paradigm.

It is important to emphasize some peculiarities of the *in vitro* system we were evaluating. The neurons were derived from transgenic newborn pups which were heterozygous. The BRI-Aβ40 transgenic construct manifests as an overexpression of Aβ40 and similarly, the BRI-Aβ42 construct induces overexpression of Aβ42 in the brain. However, even though Aβ42 overexpression in these animals was reported to manifest robust parenchymal and vascular AD-like pathology, no neuronal loss or AD phenotype was observed. *In vivo* Aβ peptide levels are governed by rates of synthesis (by proteolytic processing of APP) as well as clearance by a variety of mechanisms. Examples include lipoprotein receptor-related protein (LRP)-mediated Aβ efflux, P-glycoprotein-mediated Aβ efflux, and enzyme-mediated Aβ degradation (NEP, IDE, etc.) [22]. In cell culture, *in vivo* clearance mechanisms would be less available to neurons. Therefore, in our cell culture experimental model, there would be an expectation of progressive transgene product expression (Aβ40 or Aβ42 respectively). After exposure of these cells to TFW challenge (7 days post plating; see Materials and Methods above), these cells would secret a significant amount of Aβ40 or Aβ42 into the culture medium. This assumption is based on the original report that the BRI transmembrane protein fusion construct employed to drive transgene expression will ensure secretion of the two peptides into the extracellular space to the exclusion of any intracellular accumulation [6]. In this manner our model would expose neurons to Aβ40 or Aβ42 without other confounding factors (APP expression, protective metabolites and peptide clearance) to a large extent.

There is significant and mounting evidence that neuronal apoptosis underlies the degenerative change in AD brains [23, 24]. Therefore we chose to examine the fairly definitive marker of programmed cell death, caspases-3 activation. We cultured cortical neurons derived from these two transgenic mouse models and compared them with age-matched controls. Caspase-3 is also interesting in that the cleavage sites of this aspartate-specific protease have been found in the APP sequence and cleavage by it of the cytoplasmic tail of APP has been shown to release neurotoxic fragments that upregulate Aβ peptide synthesis and accumulation [25, 26]. Utilizing the widely used DEVD-AFC based assay for fluorescent reporting of caspases-3 activity, we found that at basal levels of TFW challenge (within minutes of withdrawing growth medium), the three cell lines had no protease activation. For all three cell lines caspase-3 activity increased with time post-challenge and peaked at 8 hours

post-challenge before beginning to drop at one day post-challenge. Profiles of both transgenic cell types remained elevated above WT levels throughout the temporal spectrum. When we performed a DNA-fragmentation based cell count aided by the dsDNA intercalating fluorescent reporter PI, we found that both transgenic cell lines (Aβ40 and 42) were markedly affected 24 hours post-TFW challenge. In contrast, WT cells remained unaffected. While this is a surprising finding given that even in WT cells, increasing caspases-3 activation was observed in temporal sequence from 0 to 24 after TFW challenge with peaks appearing in all three tested cell populations at 8 hours. However, caspases-3 activation may not spell the inevitability of death in every situation. There is also evidence that multiple factors may provide protection against both apoptosome assembly and cleaved caspases even though the apoptotic cascade may have been triggered. The idea that mitochondrial functional deficits play a role in neurodegenerative pathologies has been studied for many years yielding tantalizing information. Evidence for deficiencies of cytochrome c oxidase (COX/Complex IV) has been widely reported [29-31]. More recent investigations have shown that both of the primary amyloid β species involved in AD (1-40 and 1-42) seem to sequester in the mitochondrion, interfere with its function and are causally implicated in free radical generation [32]. Overall, it can be stated with reasonable assurance that an increase in reactive oxygen species in the neuron in parallel with mitochondrial damage is an important contributor to AD pathogenesis [33-35]. Rhd123 is attracted to the relatively high electronegative potential of mitochondrial membranes without affecting the mitochondrial electron transport chain [36]. When we stained cultured neurons with this molecular probe, it was clear that at an early post-challenge time point (4 hours in this case), WT cells exhibited robust mitochondrial potentials while both transgenic neurons had attenuation of this parameter. However, as TFW conditions progressed in time, these potentials began to decline for all three cell types with WT levels remaining somewhat above transgenic potentials throughout the measured time frame (up to 24 hours post-challenge). Why would there be an increase in mitochondrial membrane potentials (Rhd123 fluorescence correlates strongly with this parameter) in WT neurons a few hours after TFW challenge? A few years ago, Hirai and colleagues demonstrated that mitochondrial number is upregulated in AD affected human brains and that there is also compelling evidence for mitochondrial autophagy in these specimens [37]. These finding are also consistent with evidence for low levels of mitochondrial enzymes, particularly cytochrome oxidase (which has to be membrane bound to function) in the AD brain [38]. When taken as a whole, the literature is suggestive of the provocative idea that (a) normal neurons might benefit from the ability to enhance the functioning subcellular mitochondrial population in the face of stress and, (b) that neurons derived from Aβ40 and Aβ42 overexpressing cells, in contrast, might lose functional mitochondria with TFW challenge and therefore become more vulnerable to injury and death. However, more work is clearly needed to establish such a causal relationship in AD.

The pattern of apoptotic death induced by oxidative stress is a prominent feature of AD [39]. Furthermore, antioxidants like vitamin E appear to attenuate AD neurotoxicity [40]. Formation of free carbonyls and thiobarbituric acid-reactive products, an index of oxidative damage, are significantly increased in AD brain tissue compared to age-matched controls [41, 42]. We therefore were prompted to assess oxidative stress in the transgenic cells in comparison with age-matched WT neurons. We had predicted that transgenic cells would exhibit significantly higher levels of stress. When we used H2DCF; which is rapidly oxidized by free radical species to the fluorescent DCF, we observed a sharp divergence in free radical levels in transgenic neurons while WT cells remained at relatively low levels of activity over the 24 hours time frame of measurement. The departure in activity between transgenic cells and WT occurred beyond 4 hours post-TFW challenge. Thus, in part, our observations of oxidative stress are consistent with data reported by many other authors in that neurons with high Aβ peptide load face increased oxidative insult. However, we found little difference in the oxidative stress between Aβ40 and Aβ42. How can this be explained? Several AD researchers have posited that even though Aβ42 has been implicated in AD as the more amyloidogenic fragment of APP, its more numerous cousin, Aβ40 is not entirely benign either. Aβ peptide

toxicity has been observed *in vitro*, primarily after a prolonged incubation (for many hours or days) with low concentrations (~1 μM) or after short-term treatment (4–6 h) with relatively higher concentrations (20–50 μM) of Aβ1–40 [43-46]. In the last several years, many authors have reported that both Aβ1–40 and Aβ1–42 appear to induce ionic currents across artificial bilayers. These data has been widely interpreted to mean that amyloid β peptides could insert into cell membranes as aberrant ion channels [47-49]. More recently, as a partial refutation of this idea, Sokolov and colleagues have argued that instead of forming discrete ion channels, Aβ peptides could alter neuronal membrane dielectric properties, thereby inducing similar phenomena qualitatively [50]. Whatever the exact underlying mechanism is, both Aβ40 and Aβ42 appear to possess the potential to disrupt neuronal machinery. Under the added weight of nutritive challenge (ie, TFW), the vulnerabilities of neurons expressing high levels of these proteins would be heightened, perhaps to a comparable degree.

It is also possible that the lack of difference between Aβ40 and Aβ42 neurons we observed in terms of apoptotic signaling, oxidative stress and mitochondrial dysfunction, could be peculiar attributes of our experimental system. This fact can be referenced to the original report of the transgenic strains by McGowan and her colleagues in that the mice, despite abundant cortical and cerebrovascular amyloid deposition, do not exhibit an AD neurotoxic phenotype. It is obvious, therefore, that our findings require further study and extension toward a more detailed delineation of the mechanistic correlates.

Conclusions

The BRI-Aβ40 and BRI-Aβ42 transgenic murine species affords a unique opportunity to evaluate the impact of several fold increases in expression of the two key peptide fragments whose interplay is considered central to AD pathology. Because debate continues regarding which of these species is instrumentally responsible for neuronal loss in AD, it is especially important to decipher this puzzle. Our data suggests that Aβ40 and Aβ42 have similar neurotoxic properties in cultured transgenic cortical neurons, in spite of the dramatic difference in their amyloidogenic properties *in vivo*. These results seem to be consistent with the observations in humans that levels of Aβ load in the brain are not necessarily proportional to the extent of neuronal cell death in AD. The underlying mechanism for this discrepancy in amyloidogenesis and neurotoxicity by different isoforms of Aβ is unknown, although formation of dysfunctional calcium channels by Aβ could be a contributing factor. Oligomeric Aβ peptides may form abnormal ion channels (with some ionic specificity toward Ca^{2+}) that are devoid of any of the classic regulatory controls (e.g., voltage gating, ligand gating, etc.). These hypothetical channel-like structures formed by Aβ peptides could trigger cell death from multiple interconnected signaling pathways. Experiments employing classic techniques of whole-cell/membrane patch techniques are underway in our lab to test this ion channel hypothesis of Aβ toxicity in detail.

Please address all correspondences to Najeeb A. Shiwany, M.D., or Qing Guo, M.D., Ph.D., at the Department of Physiology, University of Oklahoma Health Sciences Center, Oklahoma City, OK 73104. Tel: 405-271-2226; Fax: 405-271-3181; Emails: najeeb-shirwany@ouhsc.edu, qing-guo@ouhsc.edu

References

[1] Wong CW, Quaranta V and Glenner GG. Neuritic plaques and cerebrovascular amyloid in Alzheimer disease are antigenically related. *Proc Natl Acad Sci USA* 1985;82:8729-8732.

[2] Haass C. Presenile because of presenilin: the presenilin genes and early onset Alzheimer's disease. *Curr Opin Neurol* 1996;9:254-259.

[3] Tomlinson BE, Blessed G and Roth M. Observations on the brains of non-demented old people. *J Neurol Sci* 1968;7:331-356.

[4] Tomlinson BE, Blessed G and Roth M. Observations on the brains of demented old people. *J Neurol Sci* 1970;11:205-242.

[5] Wenk GL. Neuropathologic changes in Alzheimer's disease. *J Clin Psychiatry* 2003;64 Suppl 9:7-10.

[6] McGowan E, Pickford F, Kim J, Onstead L, Eriksen J, Yu C, Skipper L, Murphy MP, Beard J, Das P, Jansen K, Delucia M, Lin WL, Dolios G, Wang R, Eckman CB, Hutton M, Hardy J and Golde T. Aβ42 is essential for parenchymal and vascular amyloid deposition in mice. *Neuron* 2005;47:191-199.

[7] Mattson MP. Pathways towards and away from Alzheimer's disease. *Nature* 2004;430: 631-639.

[8] Yankner BA, Dawes LR, Fisher S, Villa-Koaroff L, Oster-Granite ML and Neve RL. Neurotoxicity of

a fragment of the amyloid precursor associated with Alzheimer's disease. *Science* 1989;245: 417-420.

[9] LaFerla FM. Calcium dyshomeostasis and intracellular signalling in Alzheimer's disease. *Nat Rev Neurosci* 2002;3:862-872.

[10] Li WP, Chan WY, Lai HW and Yew DT. Terminal dUTP nick end labeling (TUNEL) positive cells in the different regions of the brain in normal aging and Alzheimer patients. *J Mol Neurosci* 1997;8:75-82.

[11] Brune B. Nitric oxide: NO apoptosis or turning it ON? *Cell Death Differ* 2003;10:864-869.

[12] Ikeda K, Kajiwara K, Tanabe E, Tokumaru S, Kishida E, Masuzawa Y and Kojo S. Involvement of hydrogen peroxide and hydroxyl radical in chemically induced apoptosis of HL-60 cells. *Biochem Pharmacol* 1999;57: 1361-1365.

[13] Payette DJ, Xie J and Guo G. Reduction in CHT1-mediated choline uptake in primary neurons from presenilin-1 M146V mutant knock-in mice. *Brain Res* 2007;1135:12-21.

[14] Guo Q, Fu W, Xie J, Luo H, Sells SF, Geddes JW, Bondada V, Rangnekar VM and Mattson MP. Par-4 is a mediator of neuronal degeneration associated with the pathogenesis of Alzheimer disease. *Nat Med* 1998;4:957-962.

[15] Trojanowski JQ. Neuropathological verisimilitude in animal models of Alzheimer's disease: key to elucidating neurodegenerative pathways and identifying new targets for drug discovery. *Am J Pathol* 2002;160:409-411.

[16] Thal DR, Capetillo-Zarate E, Del Tredici K and Braak H. The development of amyloid beta protein deposits in the aged brain. *Sci Aging Knowledge Environ* 2006. 2006: re1.

[17] Griffin WS, Stanley LC, Ling C, White L, Macleod V, Perrot LJ, White CL 3rd and Araoz C. Brain interleukin 1 and S-100 immunoreactivity are elevated in Down syndrome and Alzheimer disease. *Proc Natl Acad Sci USA* 1989;86: 7611-7615.

[18] McGeer PL, Akiyama H, Itagaki S and McGeer EG. Activation of the classical complement pathway in brain tissue of Alzheimer patients. *Neurosci Lett* 1989;107:341-346.

[19] Suh YH and Checler F. Amyloid precursor protein, presenilins, and alpha-synuclein: molecular pathogenesis and pharmacological applications in Alzheimer's disease. *Pharmacol Rev* 2002;54:469-525.

[20] Suzuki N, Cheung TT, Cai XD, Odaka A, Otvos L Jr, Eckman C, Golde TE and Younkin SG. An increased percentage of long amyloid beta protein secreted by familial amyloid beta protein precursor (beta APP717) mutants. *Science* 1994;264:1336-1340.

[21] Podlisny MB, Tolan DR and Selkoe DJ. Homology of the amyloid beta protein precursor in monkey and human supports a primate model for beta amyloidosis in Alzheimer's disease. *Am J Pathol* 1991;138: 1423-1435.

[22] Wang YJ, Zhou HD and Zhou XF. Clearance of amyloid-beta in Alzheimer's disease: progress, problems and perspectives. *Drug Discov Today* 2006;11:931-938.

[23] Cotman CW and Anderson AJ. A potential role for apoptosis in neurodegeneration and Alzheimer's disease. *Mol Neurobiol* 1995;10: 19-45.

[24] Johnson EM Jr. Possible role of neuronal apoptosis in Alzheimer's disease. *Neurobiol Aging* 1994;15 Suppl 2:S187-S189.

[25] Lu DC, Rabizadeh S, Chandra S, Shayya RF, Ellerby LM, Ye X, Salvesen GS, Koo EH and Bredesen DE. A second cytotoxic proteolytic peptide derived from amyloid beta-protein precursor. *Nat Med* 2000;6:397-404.

[26] Gervais FG, Xu D, Robertson GS, Vaillancourt JP, Zhu Y, Huang J, LeBlanc A, Smith D, Rigby M, Shearman MS, Clarke EE Zheng H, Van Der Ploeg LH, Ruffolo SC, Thornberry NA, Xanthoudakis S, Zamboni RJ, Roy S and Nicholson DW. Involvement of caspases in proteolytic cleavage of Alzheimer's amyloid-beta precursor protein and amyloidogenic A beta peptide formation. *Cell* 1999;97:395-406.

[27]McLaughlin B, Hartnett KA, Erhardt JA, Legos JJ, White RF, Barone FC and Aizenman E. Caspase 3 activation is essential for neuroprotection in preconditioning. *Proc Natl Acad Sci USA* 2003; 100:715-720.

[28] Adrain C and Martin SJ. The mitochondrial apoptosome: a killer unleashed by the cytochrome seas. *Trends Biochem Sci* 2001;26:390-397.

[29] Parker WD Jr, Mahr NJ, Filley CM, Parks JK, Hughes D, Young DA and Cullum CM. Reduced platelet cytochrome c oxidase activity in Alzheimer's disease. *Neurology* 1994;44: 1086-1090.

[30] Parker WD Jr, Filley CM and Parks JK. Cytochrome oxidase deficiency in Alzheimer's disease. *Neurology* 1990;40:1302-1303.

[31] Chandrasekaran K, Stoll J, Brady DR and Rapoport SI. Localization of cytochrome oxidase (COX) activity and COX mRNA in the hippocampus and entorhinal cortex of the monkey brain: correlation with specific neuronal pathways. *Brain Res* 1992;579: 333-336.

[32] Manczak M, Anekonda TS, Henson E, Park BS, Quinn J and Reddy RH. Mitochondria are a direct site of A beta accumulation in Alzheimer's disease neurons: implications for free radical generation and oxidative damage in disease progression. *Hum Mol Genet* 2006; 15:1437-149.

[33] Khan SM, Cassarino DS, Abranova NN, Keeney PM, Borland MK, Trimmer PA, Krebs CT, Bennett JC, Parks JK, Swerdlow RH, Parker WD

Jr and Bennett JP Jr. Alzheimer's disease cybrids replicate beta-amyloid abnormalities through cell death pathways. *Ann Neurol* 2000;48:148-155.

[34] Reddy PH and Beal MF. Are mitochondria critical in the pathogenesis of Alzheimer's disease? *Brain Res Brain Res Rev* 2005;49: 618-632.

[35] Swerdlow RH and Khan SM. A "mitochondrial cascade hypothesis" for sporadic Alzheimer's disease. *Med Hypotheses* 2004;63:8-20.

[36] Johnson LV, Walsh ML and Chen LB. Localization of mitochondria in living cells with rhodamine 123. *Proc Natl Acad Sci USA* 1980; 77:990-994.

[37] Hirai K, Aliev G, Nunomura A, Fujioka H, Russell RL, Atwood CS, Johnson AB, Kress Y, Vinters HV, Tabaton M, Shimohama S, Cash AD, Siedlak SL, Harris PL, Jones PK, Petersen RB, Perry G and Smith MA. Mitochondrial abnormalities in Alzheimer's disease. *J Neurosci* 2001;21:3017-3023.

[38] Wong-Riley M, Antuono P, Ho KC, Egan R, Hevner R, Liebl W, Huang Z, Rachel R and Jones J. Cytochrome oxidase in Alzheimer's disease: biochemical, histochemical, and immunohistochemical analyses of the visual and other systems. *Vision Res* 1997;37: 3593-3608.

[39] Busciglio J, Lorenzo A, Yeh J and Yankner BA. beta-amyloid fibrils induce tau phosphorylation and loss of microtubule binding. *Neuron* 1995; 14:879-888.

[40] Mark RJ, Hensley K, Butterfield DA and Mattson MP. Amyloid beta-peptide impairs ion-motive ATPase activities: evidence for a role in loss of neuronal Ca2+ homeostasis and cell death. *J Neurosci* 1995;15:6239-6249.

[41] Smith CD, Carney JM, Starke-Reed PE, Oliver CN, Stadtman ER, Floyd RA and Markesbery WR. Excess brain protein oxidation and enzyme dysfunction in normal aging and in Alzheimer disease. *Proc Natl Acad Sci USA* 1991;88: 10540-10543.

[42] Subbarao KV and Richardson JS. Iron-dependent peroxidation of rat brain: a regional study. *J Neurosci Res* 1990;26: 224-232.

[43] Blanc EM, Toborek M, Mark RJ, Hennig B and Mattson MP. Amyloid beta-peptide induces cell monolayer albumin permeability, impairs glucose transport, and induces apoptosis in vascular endothelial cells. *J Neurochem* 1997; 68:1870-1881.

[44] Suo Z, Fang C, Crawford F and Mullan M. Superoxide free radical and intracellular calcium mediate A beta(1-42) induced endothelial toxicity. *Brain Res* 1997;762: 144-152.

[45] Good TA, Smith DO and Murphy RM. Beta-amyloid peptide blocks the fast-inactivating K+ current in rat hippocampal neurons. *Biophys J* 1996;70:296-304.

[46] Salinero O, Moreno-Flores MT, Ceballos ML and Wandosell F. beta-Amyloid peptide induced cytoskeletal reorganization in cultured astrocytes. *J Neurosci Res* 1997;47:216-223.

[47] Arispe N, Rojas E and Pollard HB. Alzheimer disease amyloid beta protein forms calcium channels in bilayer membranes: blockade by tromethamine and aluminum. *Proc Natl Acad Sci USA* 1993;90:567-571.

[48] Sanderson KL, Butler L and Ingram VM. Aggregates of a beta-amyloid peptide are required to induce calcium currents in neuron-like human teratocarcinoma cells: relation to Alzheimer's disease. *Brain Res* 1997;744:7-14.

[49] Fraser SP, Suh YH and Djamgoz MB. Ionic effects of the Alzheimer's disease beta-amyloid precursor protein and its metabolic fragments. *Trends Neurosci* 1997;20:67-72.

[50] Sokolov Y, Kozak JA, Kayed R, Chanturiya A, Glabe C and Hall JE. Soluble amyloid oligomers increase bilayer conductance by altering dielectric structure. *J Gen Physiol* 2006;128: 637-647.